



# Comparing Calculated and Observed Vertical Suspended-Sediment Distributions from a Hudson River Estuary Turbidity Maximum

P. M. Orton<sup>a,b</sup> and G. C. Kineke<sup>a,c</sup>

<sup>a</sup>Marine Science Program, University of South Carolina, Columbia, SC 29208, U.S.A.

<sup>b</sup>Present address: Environmental Science and Engineering, Oregon Graduate Institute, 20000 NW Walker Rd., Beaverton, OR 97006, U.S.A.

<sup>c</sup>Present address: Department of Geology and Geophysics, Boston College, Chestnut Hill, MA 02167, U.S.A.

Received 8 April 1998 and accepted in revised form 9 November 2000

Suspended-sediment concentrations calculated using a vertical suspended-sediment distribution equation were compared to observations from a field study of the lower turbidity maximum of the Hudson River Estuary. At four stations, an instrumented tripod measured vertical profiles of suspended-sediment concentration, current velocity, salinity and temperature through a tidal cycle. Bed and suspended-sediment samples were also analysed to determine inorganic sediment size distributions. Velocities were as high as  $1.3 \text{ m s}^{-1}$ , with suspended-sediment concentrations up to  $2000 \text{ mg l}^{-1}$ . When a well-defined pycnocline existed, cross-isopycnal mixing was strongly damped (based on the gradient Richardson number). Suspended-sediment profiles were calculated with a stratification-modified Rouse equation, using (1) reference concentrations measured at 20 cm above the bed, (2) estimates of shear velocity based on the quadratic stress law, and (3) a constant sediment settling velocity of  $0.22 \text{ cm s}^{-1}$ . Differences between mean calculated and observed total suspended load for each station were  $-17$ ,  $7$ ,  $14$  and  $58\%$ , respectively. An uncertainty analysis revealed that the two parameterizations most likely to account for differences of this magnitude were those used for settling velocity and stratification. Best results were found when substituting a power law relationship for settling velocity based on suspended-sediment concentration. This demonstrates the improvement which a power law formulation can provide over the commonly used constant  $w_s$  parameterization in fine sediment environments. © 2001 Academic Press

**Keywords:** sediment transport; turbidity maximum; aggregation; stratification; tidal estuaries; Hudson River

## Introduction

In recent years, scientists and engineers have worked to improve our understanding of estuarine sediment transport because of the need to dredge shipping channels and ports to maintain commerce. Pollution studies also require an understanding of sediment transport because many contaminants have a high affinity for sediment particles (Nichols, 1986). Estuarine turbidity maxima (ETM) in particular are of interest, because they are regions with suspended-sediment concentrations 10 to 100 times greater than those upstream or seaward (Nichols & Biggs, 1985). Studies have shown that ETM exert a significant influence on the distributions of trace metals and organic contaminants in estuaries (Hamblin, 1989; e.g. Menon *et al.*, 1998).

Bottom boundary layer models provide an approach to quantifying sediment transport, relating fluid shear stresses at the bed to erosion and the turbulent diffusion of sediment. The development of these

models requires multiple parameterizations for complex processes, some of which are not fully understood. The Rouse equation (Rouse, 1937) and similar vertical suspended-sediment distribution equations (VDEs) are one-dimensional simplifications these three dimensional models. VDEs have been used to test assumptions of eddy diffusivity, sediment diffusion, sediment settling, erosion, deposition, and the effects of stratification in flume studies (Gelfenbaum & Smith, 1986; Hill *et al.*, 1988) and natural environments (Sternberg *et al.*, 1986; Hamblin, 1989; Kineke & Sternberg, 1989; Sanford & Halka, 1993). The purpose of this paper is to summarize comparisons of observed and calculated suspended-sediment concentrations from an ETM in the Hudson River Estuary, and determine the applicability of various parameterizations for this particular environment.

## Theory

VDEs can be derived from simplifications of the continuity equation for mass conservation of sediment

with a transporting fluid. Assuming conditions are horizontally uniform, steady state, and the mean vertical velocity is zero, the continuity equation reduces to an equilibrium balance of upward turbulent diffusion and sediment particle settling. With a parabolic eddy diffusivity ( $K_s$ ), and a suspended-sediment concentration ( $C$ ) boundary condition called the reference concentration ( $C_a$ ), at height above the bed  $z=z_a$ , one obtains:

$$C(z) = C_a \exp\left(\frac{w_s}{\beta} \int_{z_a}^z \frac{dz}{K_s}\right)$$

where  $K_s = \beta K_m = \kappa U_* z (1 - z/h)$  (1)

This is the Rouse Equation (Rouse, 1937), though its analytical solution is typically presented. Variables include the particle settling velocity  $w_s$ ; von Kàrmàn's constant  $\kappa$ , approximately 0.408 (Nowell, 1983); total depth  $h$ ; and shear velocity  $U^*$ , which is a convenient proxy for the horizontal shear stress at the bed,  $\tau_0$ , through the relation  $U^* = \sqrt{\tau_0/\rho}$ . The proportionality coefficient ( $\beta$ ) between diffusivity for sediment ( $K_s$ ) and momentum ( $K_m$ ) is assumed to be one (Rouse, 1937).

Similar VDEs have been developed by substituting a flux boundary condition for the reference concentration (summarized in Sanford & Halka, 1993), or using exponential ( $K_m = \kappa U_* z e^{-3z/h}$ ; Kachel & Smith, 1989) or stratification-modified (Smith & McLean, 1977) forms of eddy diffusivity. The stratification-modified form of eddy diffusivity is calculated as follows:

$$K_{strat} = \frac{K_m}{1 + \gamma_{strat} \zeta} \quad (2)$$

where  $\gamma_{strat}$  is an empirical stratification coefficient, and  $\zeta$  is a stratification correction parameter taken from a scale analysis of the turbulent kinetic energy equation:

$$\zeta = \frac{\beta Ri}{1 - \beta \gamma_{strat} Ri} \quad \text{for } Ri < Ri_{critical}$$

$$\zeta = \infty \quad \text{for } Ri \geq Ri_{critical} \quad (3)$$

The gradient Richardson number,  $Ri$ , is a measure of vertical stability based on the ratio of local density gradient, which damps turbulence, to velocity shear, which generates turbulence:

$$Ri = -\frac{g}{\rho} \frac{(\partial \rho / \partial z)}{(\partial u / \partial z)^2} \quad (4)$$

The effects of stratification are negligible until  $Ri > 0.03$ , and mixing is completely suppressed when

$Ri \geq 0.25$  (Dyer, 1986). With a value of  $\beta = 1.00$ , this critical value corresponds to an empirical stratification coefficient,  $\gamma_{strat}$  of 4.0.

### Field study

The Hudson River Estuary is a partially mixed estuary, with typical maximum tidal currents of 0.8–1.4 m s<sup>-1</sup> (Kineke & Geyer, 1995), and a mean river discharge of 550 m<sup>3</sup> s<sup>-1</sup> (Firda *et al.*, 1994). The lower estuary and study area are shown in Figure 1, with distances upstream from the Battery at New York Harbor. The estuary exhibits two ETM, one associated with the head of the salt wedge, roughly near km 60, and one in the lower part of the estuary, from km 8 to 20. The lower ETM is skewed toward the west side of the estuary, and is coincident with a large reservoir of fine sediment. Observations have shown that virtually all bed sediment settles out at slack tides, indicating that this ETM is strongly dependent on local tidal resuspension (Kineke & Geyer, 1995). Model results indicate that lateral and along-channel convergence may play a role in the long-term maintenance of the ETM and sediment reservoir (Geyer *et al.*, 1998).

The RV *Omrust* occupied anchor stations along a cross-channel transect at km 12.6 on 21, 23, 24, 25 August 1995, hereafter referred to as Stations A, B, C, and D, respectively (Figure 1). At each station, an instrumented tripod (Sternberg *et al.*, 1991) was lowered and raised from the research vessel by winch, vertically profiling the water column for the duration of a tidal cycle. Instrumentation included a CTD (Ocean Sensors, Model 200), an electromagnetic current meter (Marsh McBirney, Model 512), a fluxgate digital compass (KVH Industries), an Optical Backscatter Sensor (OBS<sup>TM</sup> D&A Instruments), and four water pumps. This allowed water column profiling of temperature, depth, salinity, horizontal velocity, and suspended-sediment concentration, for up to 55 min per hour. Near-bed measurements were made no closer to the bed than the height of the sensors on the tripod, 20 cm.

All data were averaged in 12-min intervals and 20-cm vertical increments through the water column. The calibration of the OBS output to suspended-sediment concentration followed methods described in Kineke and Sternberg (1992). The resulting 95% confidence interval for concentration data was  $\pm 3.5\%$ . Riverine background concentrations from 15–20 mg l<sup>-1</sup> were subtracted from these data. Grain size analyses were performed on bed sediment samples collected with a grab sampler on 22 August, and surface and bottom ( $z=20$  cm) suspended-sediment samples collected by the tripod. A Coulter

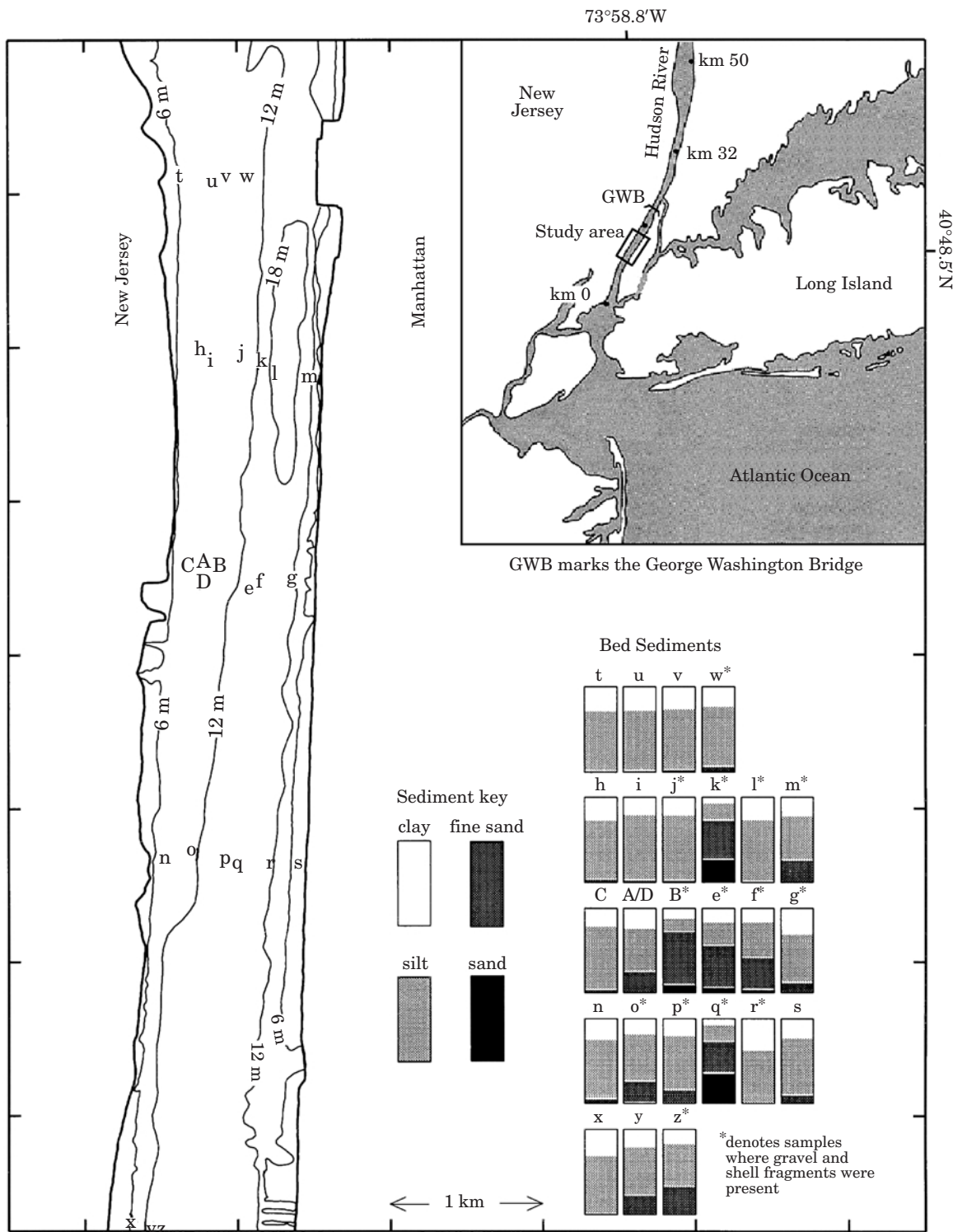


FIGURE 1. The Lower Hudson River Estuary (inset) and study area, with anchor stations marked A, B, C, D, for 21, 23, 24, 25 August. Alphabetic letters indicate grab samples obtained on 22 August 1995, with the relative concentration of each size class shown in the bottom right (clay <3.9  $\mu$ m, 3.9 <silt <62.5  $\mu$ m, 62.5 <fine sand <125  $\mu$ m, 125  $\mu$ m <sand <1 mm; T. Milligan, unpubl. data, 1996).

Counter was used for these analyses, according to methods described in Milligan and Kranck (1992). A description of bed sediments throughout the study area is given in Figure 1. Photographs were taken hourly with a Benthos-373 plankton silhouette camera.

### Suspended-sediment concentration calculations

The Rouse Equation (Equation 1) was used with the stratification modification (Equation 2) to calculate suspended-sediment concentration ( $C$ ) profiles at 12-min intervals through each day of study. For these calculations, it was necessary to obtain estimates of particle settling velocities, shear velocity, gradient Richardson number and reference concentration.

At all four stations, sediment suspensions were dominated by clay- and silt-size particles. The photographic observations demonstrated that sediment was primarily settling in aggregated form (T. Milligan, pers. comm., 1996). For fine sediments, neglecting to consider aggregation can lead to underestimation of  $w_s$  by an order or magnitude or more (Kineke & Sternberg, 1989). Preliminary analyses indicated that this leads to overestimation of  $C$  by a factor of two or more (Orton, 1996). Studies have found mean floc  $w_s$  values as low as  $0.05 \text{ cm s}^{-1}$  (Puls *et al.*, 1988). Estimates from video analyses resulted in mean  $w_s$  values as high as  $1.0 \text{ cm s}^{-1}$  (Dyer & Manning, 1999), although this method could not resolve aggregate sizes smaller than  $20 \mu\text{m}$ . Krone (1972) calculated aggregate  $w_s$  from the rate of total water column clearing at slack tides. Using the Krone method for this study, a 'characteristic' aggregate settling velocity of  $w_s = 0.22 \text{ cm s}^{-1}$  was estimated, and used in concentration calculations. This is a reasonable rough estimate of mean  $w_s$ , based on preliminary analyses of the photographic observations (T. Milligan, pers. comm., 1996).

A method for calculating shear velocity comes from the quadratic stress law (Sternberg, 1968):

$$U_*^2 = C_{D(100)} \bar{u}_{100}^2 \quad (5)$$

This involves the mean near-bed speed at  $z=100 \text{ cm}$ ,  $\bar{u}_{100}$ , and the drag coefficient,  $C_{D(100)}$ . Studies have reported  $C_{D(100)} = 2.2 \times 10^{-3}$  for muddy beds,  $2.4 \times 10^{-3}$  for unrippled sand/shell beds, and  $3.0 \times 10^{-3}$  for mud/sand beds (Dyer, 1986). Researchers involved in a simultaneous study found a value of  $C_{D(100)} = 2.5 \times 10^{-3}$  for flow over a clay/silt bed, based on high resolution velocity measurements at a mooring 2 km downstream (Trowbridge *et al.*, 1999). Based on these values, a drag coefficient of  $2.5 \times 10^{-3}$  was chosen for calculations in this study.

Profiles of gradient Richardson number (Equation 4) were calculated from velocity and total water density, which was calculated from salinity, temperature, and suspended-sediment concentration (using a sediment particle density of  $2.65 \text{ g cm}^{-3}$ ). Due to the dependence of the denominator on the square of the velocity shear, which varies greatly, there is an inherent problem with blow-up values in  $Ri$  calculations. In order to avoid complete suppression of mixing during periods with transient high  $Ri$ , values greater than  $Ri_{crit}$  were replaced with  $Ri_{crit}$  and data were smoothed with a 3-point running mean. Reference concentration,  $C_a$ , was taken from *in situ* data at  $z=20 \text{ cm}$ . This approach for  $C_a$  has been used in many previous studies (Gelfenbaum & Smith, 1986; Sternberg *et al.*, 1986; Kineke & Sternberg, 1989).

### Results

Tidal ranges increased from 0.98 to 1.15 m over the five-day period, reflecting near-neap tide conditions. River discharge was extremely low, at approximately  $100 \text{ m}^3 \text{ s}^{-1}$  (United States Geological Survey, unpubl. data, 1995). Salinity ranged from 10.3–25.0, and temperature from 24.6–27.1 °C. Maximum values of  $U_*$  were near  $4 \text{ cm s}^{-1}$ , corresponding to shear stresses ( $\tau_0$ ) of  $16 \text{ dynes cm}^{-2}$ . Table 1 and Figure 2 summarize conditions during the week of study. Figure 2 and subsequent analyses focus on Stations A and D, as these stations were at the same cross-channel location, and reflect the range of observed conditions. Total suspended load ( $Load$ ) is the vertically integrated suspended-sediment mass per unit surface area of the seabed. Percentage differences are displayed as the percentage difference between mean calculated and observed  $Load$ ,  $\Delta \overline{Load} = 100 (\overline{Load}_{calc} - \overline{Load}_{obs}) / \overline{Load}_{obs}$ .

For Station A, Figure 2 shows that stratification was generally low below the pycnocline and high within it. Suspended-sediment gradients were not large enough to lead to high near-bed density gradients and high  $Ri$  values. Observed suspended-sediment concentration ( $C_{obs}$ ) was moderately high (up to  $500 \text{ mg l}^{-1}$ ), decreased with height above the bed up to the pycnocline, and was very low above it.  $C_{calc}$  and  $Load_{calc}$  were similar to  $C_{obs}$  and  $Load_{obs}$  during increasing and maximum tidal currents, but dissimilar when currents were approaching slack tide.  $\Delta \overline{Load}$  was  $-17\%$  (Table 1), indicating that  $\overline{Load}_{calc}$  was 17% smaller than  $\overline{Load}_{obs}$ .

For Station D, there was stratification associated with a weak pycnocline during flood, but there was no pycnocline during ebb. In contrast to Station A, moderately high values of  $Ri$  were scattered

TABLE 1. Detailed observations and results, including shear velocity, maximum observed suspended-sediment concentration ( $z=20$  cm), mean observed suspended-sediment load, and mean percentage difference between mean calculated and observed load for the Rouse equation (R) and stratification-modified Rouse equation (RS)

Station, date	$U_{*max}$ ( $\text{cm s}^{-1}$ )	$C_{20max}$ ( $\text{mg l}^{-1}$ )	$\overline{Load}_{obs}$ ( $\text{g m}^{-2}$ )	$\Delta\overline{Load}$ (R) (%)	$\Delta\overline{Load}$ (RS) (%)
A, 21 August	3.9	400	234	114	-17
B, 23 August	4.2	1010	362	223	7
C, 24 August	3.6	1510	681	226	14
D, 25 August	3.8	2000	523	299	58

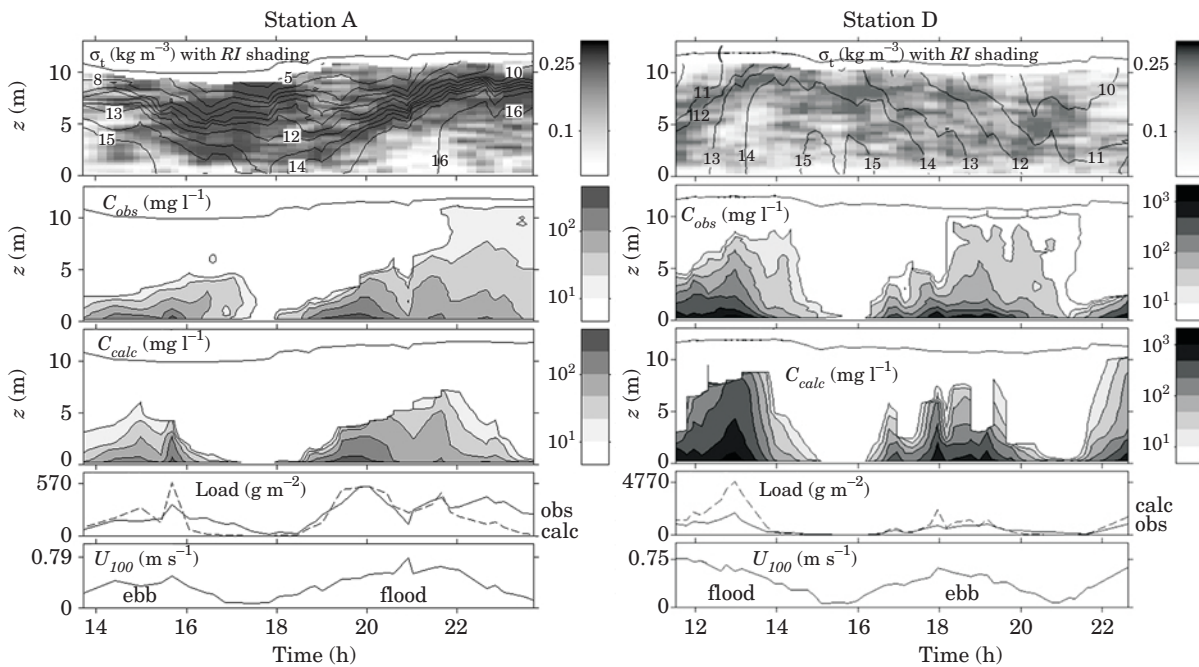


FIGURE 2. Summary of observations and results for Stations A (left; 21 August) and D (right; 25 August). From top: Density contours (does not include suspended-sediment effects on density), over gradient Richardson number shading; observed suspended sediment concentrations; calculated suspended sediment concentrations; total suspended load; and the current speed at 100 cm above the bed. Measurements and calculations are from 20 cm above the bed, up through the water column.

throughout the water column, a result of low velocity shear more than high-density gradients. Suspended-sediment gradients occasionally had a dominating effect on density gradients, producing as much as an order of magnitude increase in  $Ri$ . During flood tide,  $C_{obs}$  values were high (up to  $2000 \text{ mg l}^{-1}$ ), and did not appear to mix above the pycnocline. During ebb tide, the maximum  $C_{obs}$  was lower ( $1010 \text{ mg l}^{-1}$ ), and near-bed  $C_{obs}$  decreased rapidly with distance from the bed. However, the absence of a pycnocline appeared to allow sediment to mix to the surface, where  $C_{obs}$  was as high as  $40 \text{ mg l}^{-1}$ . Differences between  $C_{calc}$  and  $C_{obs}$  were large, reflected in the large  $\Delta\overline{Load}$  (+58%). During peak flow,  $C_{calc}$  decreased much

more slowly with distance from the bed than  $C_{obs}$ . This pattern was reversed when currents were approaching slack tide, with results similar to those for slack tides at Station A. To examine the importance of stratification, the Rouse equation was also used without the stratification modification. Concentration differences were larger, as  $C_{calc}$  exhibited more sediment mixing into the water column than with  $C_{obs}$ . Resulting  $\Delta\overline{Load}$  were 114, 223, 226, and 299%, respectively, for stations A, B, C and D.

A sensitivity analysis was conducted for concentration calculations, changing each parameter by +25%/−25%. The changes for each variable are expressed as the percentage difference in mean load,

TABLE 2. Results of the uncertainty analysis for suspended-sediment calculations

Variable, value	(source)	$\overline{\Delta Load}$ (%)
$w_{floc}=0.05 \text{ cm s}^{-1}$	(Puls <i>et al.</i> , 1988)	138
$w_{floc}=1.0 \text{ cm s}^{-1}$	(Dyer & Manning, 1999)	-72
$C_{D(100)}=2.2 \times 10^{-3}$	(summary in Dyer, 1986)	-5
$C_{D(100)}=3.0 \times 10^{-3}$	(summary in Dyer, 1986)	8
$K_m=kU_*z e^{-3z/h}$	(Kachel & Smith, 1989)	-18
$C_{20} (\pm 3.5\%)$	(OBS calibration uncertainty)	$\pm 3.5$
$Ri_{hi}$	(no de-spiking or smoothing)	-64

$\overline{\Delta Load}=100(\overline{Load_{new}} - \overline{Load_{calc}})/\overline{Load_{calc}}$ ; and are as follows  $w_s$ ,  $-18\%/+27\%$ ;  $C_{D(100)}$ ,  $+12/-10$ ;  $C_{20}$ ,  $+22/-21$ ;  $K_s$  or  $\beta$ ,  $+21/-19$ ;  $Ri_{crit}$ ,  $+9/-13$ . An 'uncertainty analysis' was also deemed valuable, as certain parameters are more highly constrained than others. Each parameter was varied over the range of values reported in the scientific literature (see preceding section), with results shown in Table 2. Uncertainty in settling velocity and the gradient Richardson number lead to the most uncertainty in  $C_{calc}$ . Using settling velocity values of 0.05 and 1.0 changed  $C_{calc}$  by +138 and -72% respectively. Using values of  $Ri$  that were not de-spiked or smoothed results in change of -64% in  $C_{calc}$ .

## Discussion

While  $\overline{\Delta Load}$  was generally low at Stations A-C, the trend toward larger and more positive values progressing from Stations A to D merits examination. A main focus of analysis was to find a parameterization change that would eliminate this progression, yet would not raise  $\overline{\Delta Load}$  for Stations A-C. Considering that  $Load_{calc}$  would need to be decreased by as much as 58% to mirror  $Load_{obs}$  at Station D, attention was focused on variables that could produce a comparable decrease in calculated concentrations. The uncertainty analysis showed that the two parameters that could account for a decrease of this magnitude were the gradient Richardson number (-64%) and settling velocity (-72%).

Figure 3 shows a profile view from Station D, during ebb tide at 18:00h. As was typical for all periods,  $Ri$  approached zero near the bed due to relatively high velocity shear.  $Ri$  was high from  $z=2$  m to the surface, reaching  $Ri_{crit}$  at  $z=7.8$  m. From that point above,  $C_{calc}$  was zero, a result of the complete absence of suspended-sediments mixing through the stratified layer. As was typically the case for periods with high  $C_{obs}$ , near-bed  $C_{calc}$  was much higher than  $C_{obs}$ , resulting in a large  $\overline{\Delta Load}$  for the profile. Two

adjustments to the stratification parameterization were considered. First, the sensitivity analysis demonstrated that adjustments to  $Ri_{crit}$  (from 0.19 to 0.31) result in small changes in  $Load_{calc}$  (-13 to +9%). Second, the smoothing of  $Ri$  was examined. While the uncertainty analysis showed that a complete absence of  $Ri$  smoothing reduced  $\overline{\Delta Load}$  substantially, the resulting time series was highly dissimilar to  $C_{obs}$ , as it was characterized by frequent abrupt decreases in  $C$  and  $Load$ . In conclusion, neither adjustment led to a substantial improvement in suspended sediment calculations.

To evaluate the constant- $w_s$  parameterization, the stratification-modified form of the Rouse equation was inverted so that observed profiles of  $C_{obs}$  could be used to solve for  $w_s$ . This is analogous to a Rouse equation inversion, where one obtains a slope-intercept equation with a slope of  $w_s/kU^*$ , and finds the best-fit slope on a plot of  $\ln z$  versus  $\ln C_{obs}$ . Near-bed data were used in this analysis ( $z \leq 2$  m), and profiles where  $C_{obs}$  was increasing with distance from the bed were not used (5% of all profiles). These  $w_s$  estimates are shown in Figure 4, which includes an empirical relation that relates settling velocity to near-bed concentration:

$$w_s = 4.6 \times 10^{-3} C_{20}^{0.45} \quad (6)$$

The exponent in Equation 6 has been shown to vary from 0.47 to 3 (Puls *et al.*, 1988; Van Leussen, 1988), and to be dependent on the location and tidal conditions during the period of study.

With aggregates, there is typically a spectrum of  $w_s$  values in any sampled volume. If the  $w_s$ -spectrum does not vary with depth, a single 'characteristic' settling velocity can be used with the Rouse equation to calculate a profile representative of a range of sediment  $w_s$  values. For the above analysis, the limited depth range (2 m) limits the effects of vertical variability in  $w_s$ -spectra. Apart from being within the range observed in previous studies, the best-fit settling

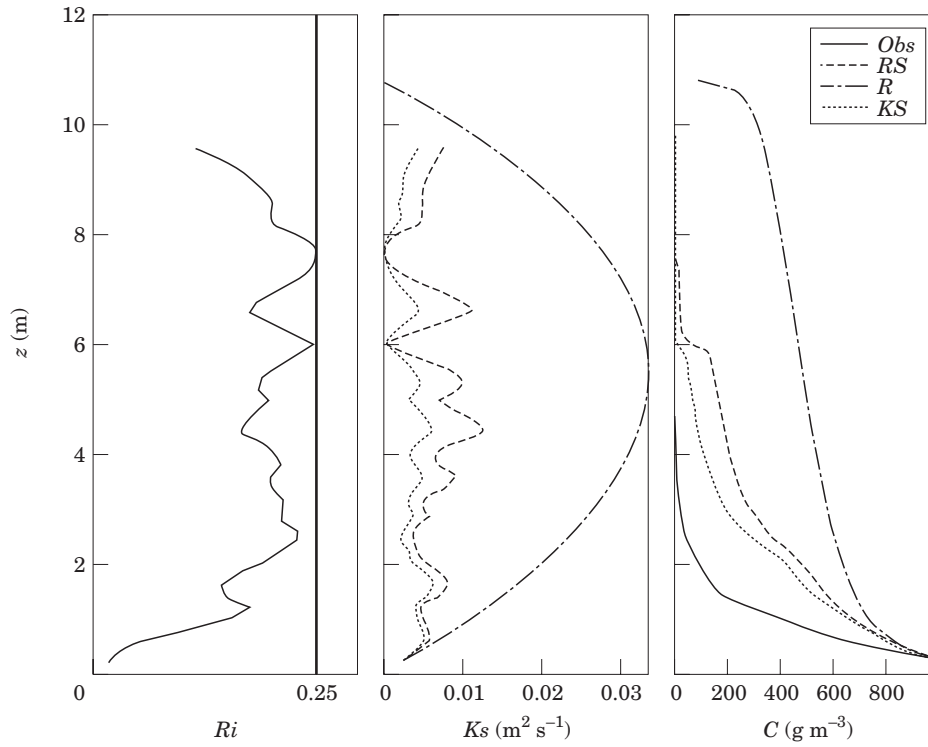


FIGURE 3. Profiles of observed gradient Richardson number (left), eddy diffusivity (middle), and suspended-sediment concentration (right). The legend describes the lines for observations (Obs), the stratified Rouse equation (RS), the Rouse equation (R), and the stratified Rouse equation with the Kachel and Smith eddy diffusivity (ks).

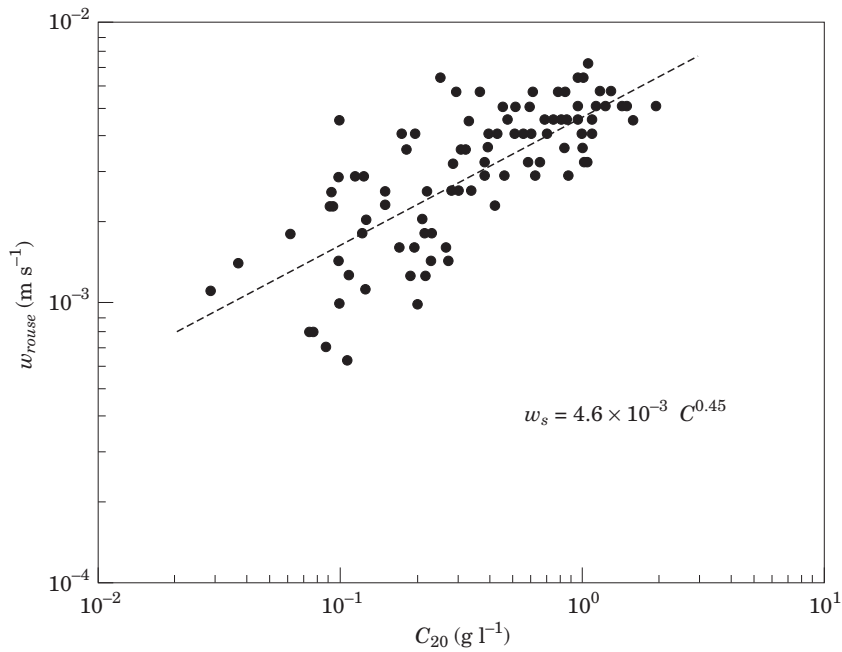


FIGURE 4. Best-fit settling velocities for all stations, with a best-fit line and equation for settling velocity as a function of the near-bed suspended-sediment concentration ( $z=20$  cm).

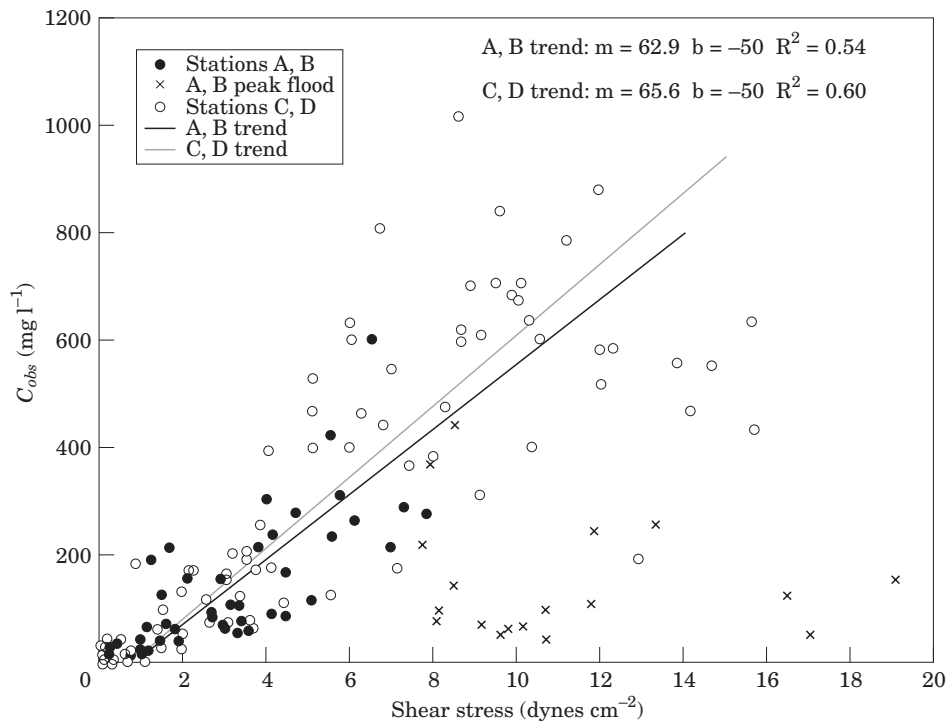


FIGURE 5. Relationship between the shear stress at the bed  $\tau_0$  and the observed near-bed suspended-sediment concentration ( $C_{obs}$ ; mean for  $20 \leq z \leq 100$  cm). The station A/B trendline does not include \*\*\* periods of peak flood currents ( $\tau_0 > 7.8$  dynes  $\text{cm}^{-2}$ ). Linear regression statistics are shown, with slope ( $m$ ), intercept ( $b$ , manually set), and  $r^2$ .

velocities form a realistic pattern where increases in  $C_{20}$  coincide with increases in near-bed  $w_s$ . This concentration-dependent  $w_s$  parameterization is attractive because it does not reduce concentrations across the board; it eliminates the trend toward increasingly positive  $\Delta \overline{Load}$  for increasing  $C_{obs}$ , while not reducing the accuracy of  $C_{calc}$  for low and intermediate levels of  $C_{obs}$ . This does not prove that these  $w_s$  estimates are accurate, or that the constant  $w_s$  parameterization was responsible for all differences between  $C_{calc}$  and  $C_{obs}$ . However, it provides the most realistic scenario for explaining these differences. It also demonstrates the improvement which a power law formulation can provide over the commonly used constant  $w_s$  parameterization in fine sediment environments.

Some limitations should be considered when interpreting these results. Sand transport is not considered, as suspensions were dominated by aggregates. If sand was being transported, virtually all remained below the closest measurement to the bed (20 cm), so had little effect on measured profile shapes. Aggregation can vary with flow conditions (Dyer & Manning, 1999), potentially limiting the use of Equation 6 during spring tides or periods of moderate and high river flow. Figure 4 does not include periods near slack tide ( $U_* < 1$   $\text{cm s}^{-1}$ ; 21% of profiles), when sediment concentration time series exhibited a phase

lag behind decreasing current velocities (Figure 2). This pattern, called settling lag, is common to most estuaries, and is a result of slow particle settling (Dyer, 1986, p. 169). This can occur at slack tides if large aggregates have settled out of the water column, leaving only small aggregates and unflocculated particles in suspension. This reflects a weakness of the Rouse equation, which is based on the assumption that sediment diffusion and settling occur quickly enough that a vertical steady state balance is rapidly attained with each incremental flow change.

Another set of periods where the Rouse equation may not be applicable was studied in more detail. A potential difficulty using the Rouse equation in ETM is that they typically contain finer bed sediments than surrounding regions (Nichols & Biggs, 1985). Due to the horizontal uniformity assumption, the Rouse equation does not account for spatial variability in flow or bed sediment characteristics. Therefore, horizontal advection of water and varying sediment compositions can lead to differences between  $C_{calc}$  and  $C_{obs}$ . Along- and across-channel differences in bed sediment composition are present in the Hudson ETM (Figure 1). An analysis of  $^{234}\text{Th}/^{7}\text{Be}$  ratios in bed- and suspended-sediment samples taken during this study suggested that 30% of suspended-sediments may have been advected from seaward of the stations

(Feng *et al.*, 1999). If bed sediment characteristics are uniform, several studies have concluded that near-bed  $C$  should be linear with respect to  $\tau_0$  (summarized in Hill *et al.*, 1988). Figure 5 shows that, excepting periods of peak flood currents at Stations A and B, this was a reasonable rough approximation. For points following the linear trend, spatial uniformity is primarily governing  $C_{obs}$ . For the 'excepted' periods, Station A and B were similar; near bed concentrations increased to maximum values 1 to 2 h after the onset of flooding tides, then began to decrease before maximum currents occurred (Figure 2, from 20.5–22.2 h). It is also worthy of note that maximum concentrations increased through the week, while maximum shear stresses remained relatively constant (Table 1). Based on these observations, it is hypothesized that there were two resuspension regimes; the first, characterized by sandy or consolidated, erosion-resistant sediment, was important during peak flood currents, early in the week ( $U_* > 2.8 \text{ cm s}^{-1}$ ; 10% of all profiles). The second, that of unconsolidated, erodible sediments, became more dominant as the week progressed. This is likely to reflect an increase in sediment trapping in the region of the ETM, with increasing tidal range. Figure 4 does not include data from the erosion-resistant periods.

### Summary and conclusions

Suspended-sediment concentration calculations were made using a stratification-modified form of the Rouse equation. Using an estimated characteristic settling velocity, calculated concentrations were similar to observed concentrations, except for periods with concentrations above  $500 \text{ mg l}^{-1}$ , and near slack tides.  $\Delta\overline{Load}$ , defined as the percentage difference between mean calculated and observed total suspended load, was  $-17$ ,  $7$ ,  $14$  and  $58\%$  for Stations A, B, C and D.

An uncertainty analysis showed that the two parameters that introduced the most uncertainty in calculated concentrations were the gradient Richardson number ( $-64\%$ ) and settling velocity ( $-72\%$ ).

Patterns suggesting settling lag or changes in bed erodability were observed for 31% of all profiles. Due to violation of Rouse equation assumptions, these profiles were not used in subsequent analyses.

There was a trend toward increasingly large and positive  $\Delta\overline{Load}$  from Station A to D, paralleling a progression toward increasing concentrations. Various parameterization adjustments were tested to remove the trend, with special consideration given to maintaining the existing accuracy during periods of low and

intermediate concentrations. The best results were found when substituting a power law form for settling velocity based on near-bed concentration.

Through comparisons of observed suspended-sediment concentrations and those calculated using vertical suspended-sediment distribution equations, valuable information can be gained regarding parameterizations commonly used in modeling studies. By continuing to work towards an understanding of the factors influencing sediment transport in turbidity maxima, we can improve the accuracy of future modeling efforts.

### Acknowledgments

The authors would like to thank Tim Milligan for sediment analyses, and Tim, John Trowbridge, and Larry Sanford for valuable comments. Thanks also to Rocky Geyer, Craig Marquette, and the crew of the RV *Onrust*. This work was funded by The Hudson River Foundation, with additional support from The University of South Carolina.

### References

- Dyer, K. R. 1986 *Coastal and Estuarine Sediment Dynamics*. Wiley-Interscience, New York, 342 pp.
- Dyer, K. R. & Manning, A. J. 1999 Observation of the size, settling velocity and effective density of flocs, and their fractal dimensions. *Journal of Sea Research* **41**, 87–95.
- Feng, H., Cochran, J. K. & Hirschberg, D. J. 1999  $^{234}\text{Th}$  and  $^7\text{Be}$  as tracers for the sources of particles to the turbidity maximum of the Hudson River Estuary. *Estuarine, Coastal and Shelf Science* **49**, 629–645.
- Gelfenbaum, G. & Smith, J. D. 1986 Experimental evaluation of a generalized suspended-sediment transport theory. In *Shelf Sands and Sandstones* (Knight, R. J. & McLean, J. R., eds). Canadian Society of Petroleum Geologists, Memoir II, pp. 133–144.
- Geyer, W. R., Signell, E. P. & Kineke, G. C. 1998 Lateral trapping of sediment in a partially mixed estuary. In *8th International Biennial Conference on Physics of Estuaries and Coastal Seas* (Dronkers & Sheffers, eds), A. A. Balkema, Rotterdam, The Netherlands, pp. 115–124.
- Hamblin, P. F. 1989 Observations and model of sediment transport near the turbidity maximum of the Upper Saint Lawrence Estuary. *Journal of Geophysical Research* **94**, 14419–14428.
- Hill, P. S., Nowell, A. R. M. & Jumars, P. A. 1988 Flume evaluation of the relationship between suspended sediment concentration and excess boundary shear stress. *Journal of Geophysical Research* **93**, 12499–12509.
- Kachel, N. B. & Smith, J. D. 1989 Sediment transport and deposition on the Washington continental shelf. In *Coastal Oceanography of Washington and Oregon* (Landry, M. R. & Hickey, B. M., eds). Elsevier, Amsterdam, pp. 287–348.
- Kineke, G. C. & Geyer, W. R. 1995 Time variation of suspended sediment in the Lower Hudson River Estuary. In *Estuaries, Bridges from Watersheds to Coastal Seas: Abstracts/Estuarine Research Federation, 13th Biennial International Conference, November 12–16, 1995, Marriott Bayfront Hotel, Corpus Christi, Texas*. Texas A&M University Sea Grant College Program, Galveston, Texas, p. 69.

- Kineke, G. C. & Sternberg, R. W. 1989 The effect of particle settling velocity on computed suspended sediment concentration profiles. *Marine Geology* **90**, 159–174.
- Kineke, G. C. & Sternberg, R. W. 1992 Measurements of high concentration suspended sediments using the optical backscatterance sensor. *Marine Geology* **108**, 253–258.
- Krone, R. B. 1972 *A field study of flucculation as a factor in estuarial shoaling processes*. Technical Bulletin No. 19, Committee on Tidal Hydraulics, United States Army Corps of Engineers, Vicksburg, Mississippi, 107 pp.
- Menon, M. G., Gibbs, R. J. & Phillips, A. 1998 Accumulation of muds and metals in the Hudson River estuary turbidity maximum. *Environmental Geology* **34**, 214–222.
- Milligan, T. G. & Kranck, K. 1992 Electro-resistance particle size analysers. In *Theory, Methods and Applications of Particle Size Analysis* (Syvitski, J. P. M., ed.). Cambridge University Press, N.Y., pp. 109–118.
- Nichols, M. N. 1986 Effects of fine sediment resuspension in estuaries. In *Estuarine Cohesive Sediment Dynamics* (Mehta, A. J., ed.). Springer-Verlag, New York, pp. 5–42.
- Nichols, M. N. & Biggs, R. B. 1985 Estuaries. In *Coastal Sedimentary Environments* (Davis, R. A., Jr., ed.). Springer-Verlag, New York, pp. 77–186.
- Nowell, A. R. M. 1983 The benthic boundary layer and sediment transport. *Reviews in Geophysics and Space Physics* **21**, 1181.
- Orton, P. M. 1996 *Evaluating the applicability of vertical suspended-sediment distribution equations in an estuarine turbidity maximum*. M.S. thesis, The University of South Carolina, 49 pp.
- Puls, W., Kuehl, H. & Heymann, K. 1988 Settling velocity of mud flocs: results of field measurements in the Elbe Estuary. In *Physical Processes in Estuaries* (Dronkers, J. & Van Leussen, W., eds). Springer-Verlag, New York, pp. 404–426.
- Rouse, H. 1937 Modern conceptions of the mechanics of fluid turbulence. *Transactions of the American Society of Civil Engineers* **102**, 463–541.
- Sanford, L. P. & Halka, J. P. 1993 Assessing the paradigm of mutually exclusive erosion and deposition of mud, with examples from upper Chesapeake Bay. *Marine Geology* **114**, 37–57.
- Smith, J. D. & McLean, S. R. 1977 Spatially averaged flow over a wavy surface. *Journal of Geophysical Research* **82**, 1735–1746.
- Sternberg, R. W. 1968 Friction factors in tidal channels with differing bed roughness. *Marine Geology* **6**, 243–260.
- Sternberg, R. W., Cacchione, D. A., Drake, D. E. & Kranck, K. 1986 Suspended sediment transport in an estuarine tidal channel within San Francisco Bay, California. *Marine Geology* **71**, 237–258.
- Sternberg, R. W., Kineke, G. C. & Johnson, R. V., II 1991 An instrument system for profiling suspended sediment, and fluid and flow conditions in shallow marine environments. *Continental Shelf Research* **11**, 109–122.
- Trowbridge, J. H., Geyer, W. R., Bowen, M. M. & Williams, A. J. 1999 Near-bottom turbulence measurements in a partially mixed estuary: Turbulent energy balance, velocity structure, and along-channel momentum balance. *Journal of Physical Oceanography* **29**, 3056–3072.
- Van Leussen, W. 1988 Aggregation of particles, settling velocity of mud flocs: A review. In *Physical Processes in Estuaries* (Dronkers, J. & van Leussen, W., eds). Springer Verlag, New York, pp. 347–403.